Supplementary Information for "Spin-lattice and electron-phonon coupling in $3d/5d$ hybrid Sr_3NiIrO_6"

Kenneth R. O'Neal,[1] Arpita Paul,[2] Amal al-Wahish,[1] Kendall D. Hughey,[1] Avery L. Blockmon,[1] Xuan Luo,[3,4,5] Sang-Wook Cheong,[3,4,6] Vivien Zapf,[7] Craig V. Topping,[8] John Singleton,[7] Mykhalo Ozerov,[9] Turan Birol,[10] and Janice L. Musfeldt[1,11]

[1]*Department of Chemistry, University of Tennessee, Knoxville, Tennessee 37996, USA*

[2]*Department of Chemical Engineering and Materials Science, University of Minnesota, Minneapolis, MN 55455, USA*

[3]*Max Planck POSTECH/Korea Research Initiative, Pohang University of Science and Technology, Pohang 37673, Korea*

[4]*Key Laboratory of Pohang Emergent Materials, Pohang Accelerator Laboratory, Pohang 37673, Korea*

[5]*Key Laboratory of Materials Physics, Institute of Solid State Physics, Chinese Academy of Sciences, Hefei, 230031, China*

[6]*Rutgers Center for Emergent Materials and Department of Physics and Astronomy, Rutgers University, Piscataway, New Jersey 08854, USA*

[7]*National High Magnetic Field Laboratory (NHMFL), MS E536, Los Alamos National Laboratory, New Mexico, 87545, USA*

[8]*School of Physics & Astronomy, University of St Andrews, North Haugh, St Andrews, KY16 9SS, United Kingdom*

[9]*National High Magnetic Field Laboratory, Tallahassee, Florida 32310, USA*

[10]*Chemical Engineering and Materials Science, University of Minnesota, Minneapolis, MN 55455, USA*

[11]*Department of Physics and Astronomy, University of Tennessee, Knoxville, Tennessee 37996, USA*

(Dated: July 18, 2019)

Structure, infrared spectra, and mode assignments of Sr_3NiIrO_6 and Sr_3CuIrO_6

Sr_3NiIrO_6 and the Cu analog belong to a family $A_3BB'O_6$ materials (A = alkaline-earth metal, B and B' = transition metal) [S1–S3] that crystallize in quasi-one-dimensional chain structures. The chains form a triangular lattice within the ab plane [Fig. S1 (a)], leading to complex, frustrated magnetism [S1, S4–S6]. While the chain of the Ni system is linear [Fig. S1 (b)], the Cu material exhibits a zigzag pattern [Fig. S1 (c)]. Transition metal site substitution therefore reduces symmetry and, as we shall see, modifies the vibronically-coupled phonon that activates the Ir excitations. The lower symmetry of Sr_3CuIrO_6 (space group $C12/c1$) compared to Sr_3NiIrO_6 ($R\bar{3}c$) is evidenced by the greater number of features in the infrared spectra [Figure S2]. The lack of large frequency shifts with decreasing temperature in Sr_3NiIrO_6 indicates weak spin-lattice coupling across the 75 K ordering and 15 K freezing temperatures [S1, S5].

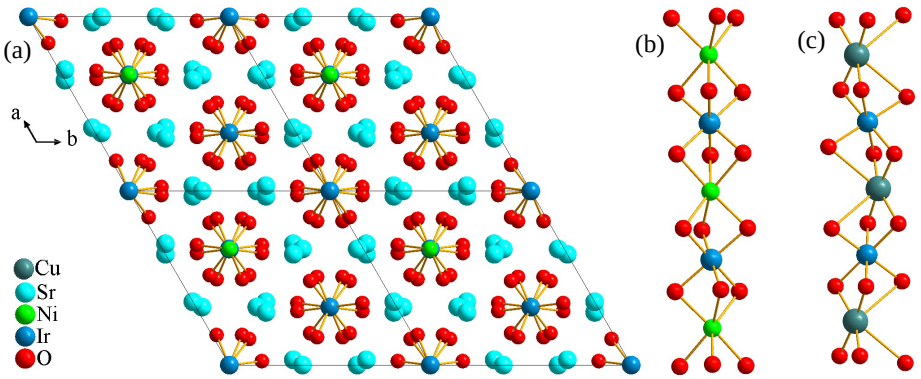

FIG. S1. Crystal structure of Sr_3NiIrO_6 viewed (a) along and (b) perpendicular to the chain direction. The chain of Sr_3NiIrO_6 (b) is linear while the Cu analog (c) is zigzag.

We assign the phonons of Sr_3NiIrO_6 and Sr_3CuIrO_6 based upon our lattice dynamics calculations (Tables S1 and S2). For completeness, we also tabulate the calculated Raman-active phonon frequencies and symmetries for both systems (Tables S3 and S4). This reveals the effect of transition metal site substitution.

Animated displacement patterns of Sr_3NiIrO_6

In Sr_3NiIrO_6, three phonons (133, 310, and 534 cm^{-1}) are sensitive to magnetic field while another (177 cm^{-1}) engages in electron-phonon coupling. The displacement patterns are described and illustrated in the main text. We also provide animations [S7] to better visualize

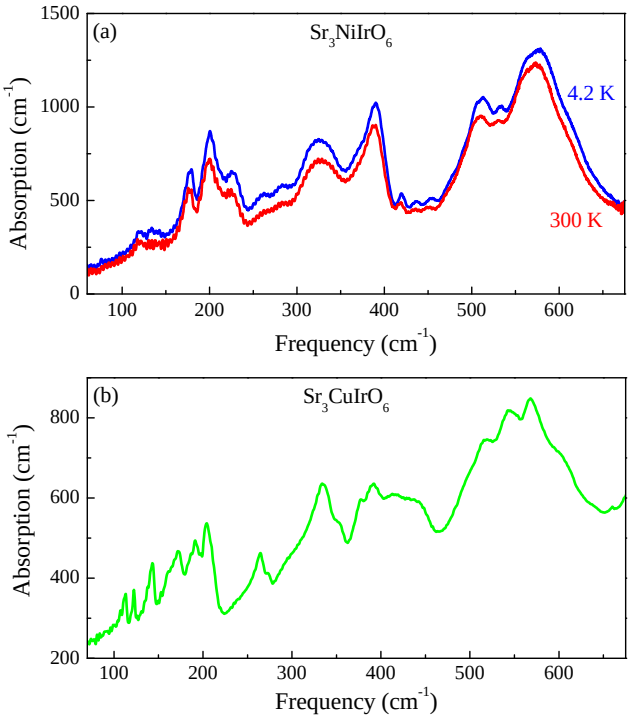

FIG. S2. (a) Infrared absorption of polycrystalline Sr_3NiIrO_6 at 300 and 4.2 K. Spectra are offset for clarity. (b) Infrared spectrum of polycrystalline Sr_3CuIrO_6 at room temperature. Transition metals substitution (from Ni $\rightarrow$ Cu) clearly lowers the symmetry.

the motions. For each phonon, there is a close-up animation of the intra-chain motions (named as the frequency and symmetry of the mode followed by "perp to chain") and a wider view that highlights the inter-chain displacements (similarly named, but ending with "along chain"). The atom colors correspond to those used in Fig. S1.

The intra-chain motions for the most important phonons are described in the main text, and a full summary is given in Table S1. As a reminder, the 310 and 534 cm^{-1} modes are dominated by O motion and strongly affect the Ir environment. The 133 cm^{-1} mode consists of Ni motion along c and Sr movement, which modulates the Ir environment as a second-order effect. Importantly, each of these modes also has inter-chain character as evident in the wide view animations. For the 133 cm^{-1} mode, the Sr atoms vibrate between the chains and should strongly affect the inter-chain interactions. The O motion of the 310 and 534 cm^{-1} phonons also modulates the exchange between chains. The magnetic field-induced frequency shifts of these modes suggests that inter-chain interactions play an important role in the magnetic properties of Sr_3NiIrO_6. Their presence (or absence) is also important for validating the working model for the ultra-high coercivity. The 177 cm^{-1} phonon that engages in electron-phonon coupling, on the other hand, consists of in-phase, in-plane motion of the chain units against counter-motion of the Sr centers. As emphasized in the main text, the vibronically-active phonon does not engage in spin-lattice coupling.

TABLE S1. Summary of the symmetries and frequencies of infrared-active phonons of Sr_3NiIrO_6. Displacements are given for the important modes.

Symmetry	Experimental Frequency (cm^{-1})	Theoretical Frequency (cm^{-1})	Mode Assignment
A_{2u}	-	116	Chains moving along c against Sr motion
E_u	120	119	Sr out-of-plane motion
E_u	-	125	Ni left, Sr out-of-plane
A_{2u}	133	137	Ni along c, Sr in-plane
E_u	142	142	Ni left, Ir right
E_u	177	170	Chains moving in-plane against Sr motion
E_u	201	188	Ni out-of-phase motion along c
A_{2u}	227	251	Ni up, Ir down
A_{2u}	260	277	IrO_6 breathing
E_u	284	287	O-Ir-O bending
E_u	310	302	O-Ir-O bending
A_{2u}	330	365	O-Ir-O bending
E_u	370	371	O-Ir-O bending
E_u	389	381	O-Ir-O bending
	420		
	436		
	454		
E_u	510	536	Ir-O stretching
A_{2u}	534	549	Ir-O stretching
E_u	577	570	Ir-O stretching

TABLE S2. Summary of the experimentally observed and theoretically predicted infrared phonon frequencies and symmetries of Sr_3CuIrO_6. Nearly-degenerate frequencies for some modes makes exact assignments difficult due to the polycrystalline sample measured here, so we list candidate assignments for each symmetry.

Experimental Frequency (cm^{-1})	Theoretical A_u Frequency (cm^{-1})	Theoretical B_u Frequency (cm−1)
	103	102
108		106
113	122	115
122	132	130
142	146	
172	150	164
191	182	168
204	195	192
264		252
273	278	261
	318	314
335	334	328
354	364	361
377	370	
391		396
415		429
441	474	
518	500	506
545	533	522
568	554	533

TABLE S3. Symmetries and calculated frequencies for the Raman-active modes of Sr_3NiIrO_6.

Symmetry	Frequency (cm^{-1})	Symmetry	Frequency (cm^{-1})
E_g	99	A_{1g}	243
A_{1g}	123	E_g	323
E_g	128	E_g	356
E_g	154	A_{1g}	399
E_g	175	E_g	514
E_g	184	A_{1g}	648

TABLE S4. Symmetries and calculated frequencies for the Raman-active modes of Sr_3CuIrO_6.

Symmetry	Frequency (cm^{-1})	Symmetry	Frequency (cm^{-1})
B_g	100	B_g	253
A_g	106	A_g	283
A_g	112	B_g	308
B_g	114	A_g	319
A_g	124	B_g	339
B_g	128	A_g	365
B_g	141	B_g	366
A_g	144	B_g	412
B_g	165	A_g	441
A_g	177	A_g	520
B_g	179	B_g	548
B_g	182	A_g	566
B_g	193	B_g	567
A_g	206	B_g	591
A_g	234	A_g	623

Spin-phonon coupling in Sr_3NiIrO_6

First principles calculation have been used extensively to quantitatively predict the strength of spin-phonon coupling parameters. However, the complicated structure of Sr_3NiIrO_6 woth two magnetic species and very strong spin orbit coupling makes this an impractical task. For example, the full spin-phonon Hamiltonian that takes into account both the anisotropic exchange and the spin-orbit induced antisymmetric Dzyaloshinskii-Moriya interaction along a Ni–Ir chain can be written as

$$\mathcal{H} = \sum_{i,j,\alpha} J_{i,j,\alpha} S_{i,\alpha} S_{j,\alpha} + \sum_{i} K_i S_{i,z}^2 + \sum_{n} \frac{1}{2} k_n u_n^2 + \sum_{n} u_n \sum_{i,j,\alpha} \lambda_{i,j,\alpha,n} S_{i,\alpha} S_{j,\alpha} + \sum_{n} u_n \sum_{i,j} \vec{\gamma}_n \cdot \left(\vec{S}_i \times \vec{S}_j \right) \tag{1}$$

where the i, j indices are for the Ni and Ir atoms, α is for the Cartesian directions, and the n index is for the phonon modes. $\vec{S}_i$ is the total magnetic moment of each ion, and u_n is the amplitude of the nth normal phonon mode's displacement. The first three terms are the anisotropic symmetric exchange [S8], single ion anisotropy, and phonon energy, respectively. The fourth term is an expansion of the spin-phonon coupling that is commonly used for simple Heisenberg exchange [S9, S10]. The last term is the Dzyaloshinkii-Moriya (DM) interaction induced by symmetry lowering phonon displacements. So, $\vec{\gamma}_n$ is another type of spin-phonon coupling parameter that leads to tilting of magnetic moments. The spin-phonon coupling parameter $\lambda_{i,j,\alpha,n}$ is related to the derivative of exchange parameter $J_{i,j,\alpha}$ with respect to the mode amplitude u_n. In the undistorted structure, DM interaction is not permitted, so the DM vector $\vec{d}$ is proportional to the lattice displacement to the lowest order, $\vec{d} \sim u_n \vec{\gamma}_n$, which gives rise to the last term. Obtaining values of all coefficients $J_{i,j,\alpha}$, K_i, k_n, $\lambda_{i,j,\alpha,n}$, and $\vec{d}_n$ requires a large number of DFT calculations in various crystal structures, which correspond to different displacement patterns according to u_n, and different magnetic configurations. This is technically not possible for a complex system such as Sr_3NiIrO_6. Even stabilizing magnetic configurations away from the ground state is challenging. For this reason, we take a simpler approach to estimate the relative strength of spin-phonon coupling of different modes - as explained in the main text. This more intuitive approach involves displacing the atoms according to specific u_n's, and predicting the ground state magnetic configuration using first principles DFT. While limited, this approach gives an estimate of the relative magnitude of $\vec{\gamma}$ for different modes; and hence point to the vibrational modes that have stronger effects on the magnetic exchange pathways.

Vibronic coupling analysis of Ir on-site excitations in Sr_3CuIrO_6

Figure S3 (a) displays the absorption of Sr_3CuIrO_6 in the region of the Ir^{4+} on-site excitations. Quantifying the oscillator strength as a function of temperature and fitting it with the model discussed in the main text yields a coupling phonon frequency of 285 cm^{-1} [Fig. S3 (b)]. The infrared spectrum [Fig. S3 (c)] reveals a likely candidate for the coupled mode. The displacement [Fig. S3 (d)] contains mostly O motion around the Ir center. Interestingly, this mode is not a simple analog of the activating phonon in Sr_3NiIrO_6, which consists of Ni and Sr motions. This is most likely due to different local environments of the Ir centers stemming from the chain configurations [Fig. S1 (b,c)]. Transition metal site substitution therefore plays an important role in determining which phonon will activate the Ir on-site excitation. Table 1 in the main text compares the crystal field parameters and the coupling phonon frequency of the Cu analog with those of Sr_3NiIrO_6. We anticipate that these parameters will be useful in establishing structure-property relationships within the $Sr_3BB'O_6$ family of materials.

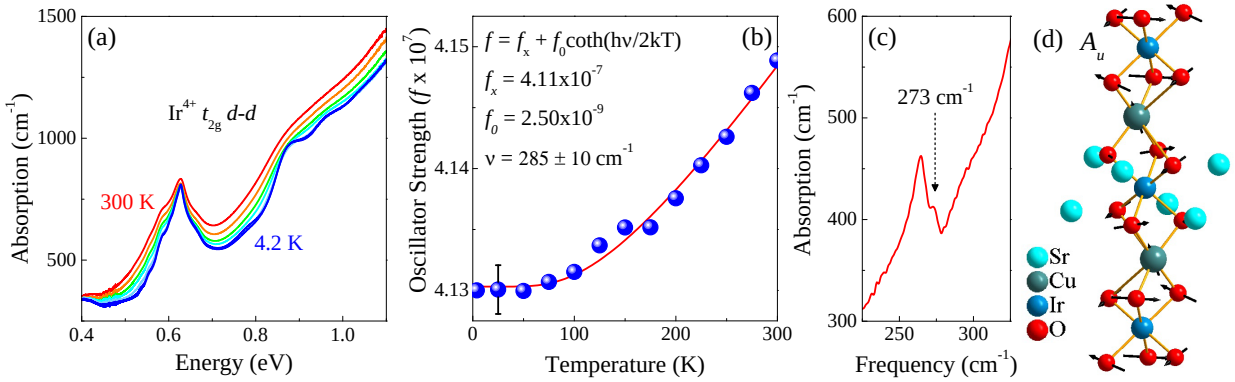

FIG. S3. (a) Optical absorption of Sr_3CuIrO_6 as a function of temperature in the vicinity of the Ir on-site d-to-d excitations. (b) Oscillator strength analysis using the indicated vibronic coupling model, where ν is the coupled phonon frequency extracted from the analysis. (c) The infrared spectrum shows phonons near the extracted ν value. (d) Calculated mode displacement pattern for the vibronically-coupled phonon.

[S1] Mikhailova, D., Schwarz, B., Senyshyn, A., Bell, A. M. T., Skourski, Y., Ehrenberg, H., Tsirlin, A. A., Agrestini, S., Rotter, M., Reichel, P., Chen, J. M., Hu, Z., Li, Z. M., Li, Z. F.,

& Tjeng, L. H. Magnetic properties and crystal structure of Sr_3CoIrO_6 and Sr_3NiIrO_6. *Phys. Rev. B* **86**, 134409 (2012).

[S2] Stitzer, K. E., Henley, W. H., Claridge, J. B., zur Loye, H. C., & Layland, R. C. Sr_3NiRhO_6 and Sr_3CuRhO_6 - Two new one-dimensional oxides. Magnetic behavior as a function of structure: Commensurate vs incommensurate. *J. Solid State Chem.* **164**, 220–229 (2002).

[S3] Nguyen, T. N. & zur Loye, H.-C. A family of one-dimensional oxides: Sr_3MIrO_6 (M = Ni, Cu, Zn): Structure and magnetic properties. *J. Solid State Chem.* **117**, 300–308 (1995).

[S4] Flahaut, D., Hébert, S., Maignan, A., Hardy, V., Martin, C., Hervieu, M., Costes, M., Raquet, B., & Broto, J. M. A magnetic study of the one dimensional Sr_3NiIrO_6 compound. *Eur. Phys. J. B* **35**, 317–323 (2003).

[S5] Lefrançois, E., Chapon, L. C., Simonet, V., Lejay, P., Khalyavin, D., Rayaprol, S., Sampathkumaran, E. V., Ballou, R., & Adroja, D. T. Magnetic order in the frustrated Ising-like chain compound Sr_3NiIrO_6. *Phys. Rev. B* **90**, 014408 (2014).

[S6] Toth, S., Wu, W., Adroja, D. T., Rayaprol, S., & Sampathkumaran, E. V. Frustrated Ising chains on the triangular lattice in Sr_3NiIrO_6. *Phys. Rev. B* **93**, 174422 (2016).

[S7] Http://henriquemiranda.github.io/phononwebsite/phonon.html.

[S8] Birol, T., Haule, K., & Vanderbilt, D. Nature of the magnetic interactions in Sr_3NiIrO_6. *Phys. Rev. B* **98**, 134432 (2018).

[S9] Birol, T., Benedek, N. A., Das, H., Wysocki, A. L., Mulder, A. T., Abbett, B. M., Smith, E. H., Ghosh, S., & Fennie, C. J. The magnetoelectric effect in transition metal oxides: Insights and the rational design of new materials from first principles. *Curr. Opin. Solid State Mater. Sci.* **16**, 227–242 (2012).

[S10] Wysocki, A. L. & Birol, T. Magnetically induced phonon splitting in ACr_2O_4 spinels from first principles. *Phys. Rev. B* **93**, 134425 (2016).